Available online at www.sciencedirect.com

ScienceDirect

Developmental Biology 306 (2007) 584–598

DEVELOPMENTAL BIOLOGY

www.elsevier.com/locate/ydbio

A targeted deletion/insertion in the mouse *Pcsk1* locus is associated with homozygous embryo preimplantation lethality, mutant allele preferential transmission and heterozygous female susceptibility to dietary fat

Majambu Mbikay [a,b,*], Gilles Croissandeau [a,1], Francine Sirois [a,1], Younes Anini [a], Janice Mayne [a], Nabil G. Seidah [c], Michel Chrétien [a,b]

[a] *Ottawa Health Research Institute and The Ottawa Hospital, Ottawa, Ontario, Canada*
[b] *Department of Biochemistry, Microbiology and Immunology, University of Ottawa, Ottawa, Ontario, Canada*
[c] *Biochemical Neuroendocrinology Laboratory, Clinical Research Institute of Montreal, Montreal, Quebec, Canada*

Received for publication 27 September 2006; revised 2 March 2007; accepted 27 March 2007
Available online 1 April 2007

Abstract

Proprotein convertase 1 (PC1) is a neuroendocrine proteinase involved in the proteolytic activation of precursors to hormones and neuropeptides. To determine the physiological importance of PC1, we produced a mutant mouse from embryonic stem cells in which its locus (*Pcsk1*) had been inactivated by homologous recombination. The inactivating mutation consisted of a 32.7-kb internal deletion and a 1.8 kb insertion of the bacterial neomycin resistance gene (*neo*) under the mouse phosphoglycerate kinase 1 protein (PGKneo). Intercross of $Pcsk1^{+/-}$ mice produced no $Pcsk1^{-/-}$ offspring or blastocysts; in addition, more than 80% of the offspring were $Pcsk1^{+/-}$. These observations suggested that the mutation caused preimplantation lethality of homozygous embryos and preferential transmission of the mutant allele. Interestingly, RT–PCR analysis on RNA from endocrine tissues from $Pcsk1^{+/-}$ mice revealed the presence of aberrant transcripts specifying the N-terminal half of the PC1 propeptide fused to *neo* gene product. Mass spectrometric profiles of proopiomelanocortin-derived peptides in the anterior pituitary were similar between $Pcsk1^{+/-}$ and $Pcsk1^{+/+}$ mice, but significantly different between male and female mice of the same genotype. Relative to their wild-type counterparts, female mutant mice exhibited stunted growth under a low fat diet, and catch-up growth under a high-fat diet. The complex phenotype exhibited by this *Pcsk1* mutant mouse model may be due to PC1 deficiency aggravated by expression of aberrant gene products from the mutant allele.

Keywords: Proprotein convertase; PC1; *Pcsk1*; Genetic deficiency; Preimplantation embryonic lethality; Transmission ratio distortion

Introduction

PC1, also known as PC3 (Smeekens et al., 1991) or SPC3 (Steiner, 1998), belongs to a family of serine proteinases that activate secretory precursor proteins by cleavages after selected pairs of basic residues (Seidah and Chretien, 1999; Steiner, 1998). In mouse, its *Pcsk1* locus maps to chromosome 13 (Seidah et al., 1991). The gene has 15 exons and 14 introns (Ftouhi et al., 1994). It is transcribed into two major mRNA isoforms of 2.8 and 4.4 kb differing in their 3′ untranslated regions (UTR) (Seidah et al., 1991) (Ftouhi et al., 1994). These transcripts are primarily found in neuroendocrine cells (Schäfer et al., 1993; Seidah et al., 1991, 1994; Zheng et al., 1994). They are translated in the endoplasmic reticulum (ER) into a 88-kDa proPC1; the zymogen gets converted in the ER and the Golgi to a 74-kDa form by autocatalytic removal of the prodomain; the mature enzyme is then sorted into secretory granules where it is further processed to its fully active form of 66-kDa by excision of a C-terminal fragment (Benjannet et al., 1993). The pro-domain may promote the proper folding of proPC1 and its exit from the ER, as demonstrated for other PCs (Anderson et al.,

* Corresponding author. Ottawa Health Research Institute, 725 Parkdale Avenue, Room 117-1, Ottawa, Ontario, Canada K1Y 4E9. Fax: +1 613 761 4355.
E-mail address: mmbikay@ohri.ca (M. Mbikay).
[1] These two authors have equally contributed to this work.

0012-1606/$ - see front matter © 2007 Elsevier Inc. All rights reserved.
doi:10.1016/j.ydbio.2007.03.523

2002; Muller et al., 2000; Rehemtulla et al., 1992); it has also been shown to inhibit PC1 enzymatic activity (Boudreault et al., 1998; Lee et al., 2004). The P domain stabilizes the catalytic domain of the enzyme (Ueda et al., 2003). The C-terminal domain has been implicated in partial inhibition of PC1 activity as well as in its sorting into secretory granules (Jutras et al., 1997, 2000).

The related proteinase PC2 is often found in the same granules (Kurabuchi and Tanaka, 2002; Malide et al., 1995; Marcinkiewicz et al., 1994; Takumi et al., 1998). The activities of the two convertases are influenced by resident granin-like proteins: proSAAS, a competitive PC1-specific inhibitor (Basak et al., 2001; Fricker et al., 2000; Qian et al., 2000) and pro7B2, a PC2-specific chaperone and inhibitor (Benjannet et al., 1995; Braks and Martens, 1994; Martens et al., 1994; Mbikay et al., 2001; Muller et al., 1997).

PC1 and PC2 often process the same substrates, but with cleavage site preferences. Their substrates are mostly prohormones and proneuropeptides (Seidah and Chretien, 1999). Proopiomelanocortin (POMC) and proinsulin are the best studied of these substrates. In the anterior lobe (AL) of the pituitary, POMC is processed primarily into adrenocorticotropic hormone (ACTH) and β-lipotropic hormones (βLPH); in the neurointermediate lobe (NIL), ACTH is further processed to α-melanocyte-stimulating hormone (α-MSH) and CLIP; and βLPH to βMSH and β-endorphin (βEND) (Chrétien and Seidah, 1981). PC1 is most abundant in the AL; and PC2 most abundant in the NIL (Marcinkiewicz et al., 1993; Seidah et al., 1990, 1991). Accordingly, using co-transfected cells, it was shown that PC1 converts POMC to peptides found in the AL and PC2 to those found in the NIL (Benjannet et al., 1991; Seidah et al., 1990; Zhou et al., 1993). PC1 cleaves proinsulin after KR^{31-32} pair joining the B and C peptides, while PC2 does it after the KR^{61-62} pair joining the C and A peptides (Smeekens et al., 1992).

Two human cases of genetic PC1 deficiency have been reported (Jackson et al., 1997, 2003). The first patient suffered from massive obesity at birth and, as an adult, exhibited hypogonadotropic hypogonadism. After treatment with gonadotropin-releasing hormone (GnRH), she conceived but developed gestational diabetes mellitus associated with increased circulating levels of des-61, 62 proinsulin, suggesting that proinsulin was cleaved by PC2 after the KR^{60-61} pair, but not by PC1 after the RR^{30-31} pair. Genetic analyses revealed that the patient was a *PCSK1* compound heterozygote carrying, on one allele, a splicing mutation that leads to the production of a truncated PC1 and, on the other allele, a missense mutation that causes a G483R substitution in the P domain of the enzyme and retention of the latter in the ER. POMC-derived peptides resulting from incomplete processing were detected in the patient's serum (Jackson et al., 1997). The second patient, an infant affected by obesity at birth and postnatal gastrointestinal dysfunctions, was posthumously identified to be a compound heterozygous for Ala213del and Glu250stop PC1 mutations (Jackson et al., 2003).

A mouse model of heritable PC1 deficiency was generated by Zhu et al. (2002b) by targeted ablation of the promoter and the first exon of the *PC1* gene. Intercross of $Pcsk1^{+/-}$ mice produced offspring of all three genotypes, but homozygous nulls were underrepresented, suggesting partial prenatal mortality. Neonatal mortality of nulls was also observed. Surviving $Pcsk1^{-/-}$ mice exhibited smaller birth weight and stunted growth; they also suffered from gastrointestinal dysfunctions as manifested by a moist texture of their stools. Growth retardation was due to impaired processing of hypothalamic growth hormone-releasing hormone, resulting in less plasma growth hormone and insulin-like growth factor (IGF-1). POMC and proinsulin processing was also impaired in these mice (Dey et al., 2004; Marzban et al., 2004; Zhu et al., 2002a,b). A chemically induced N222D mutation in the catalytic domain of PC1 was recently described in mouse: homozygous mutants develop obesity and glucose intolerance associated with impaired processing of central and peripheral prohormones and proneuropeptides (Lloyd et al., 2006).

Here, we describe another model of PC1 heritable deficiency, generated by substituting a 32.7-kb internal region of its gene with a 1.8 kb heterologous gene. Homozygotes for this mutation died during preimplantation embryonic development; the mutant allele was preferentially transmitted by heterozygous parents and, in female heterozygotes, weight gain with age was influenced by dietary fat content.

Materials and methods

Pcsk1 disruption vector

Genomic DNA was extracted from the R1 embryonic stem (ES) cells established from 129Sv mice. Fragments used as *Pcsk1* homology regions in the disruption vector were amplified by PCR from this DNA and cloned into a vector previously used to disrupt the *Pcsk4* locus (Mbikay et al., 1997). The 5′ homology amplicon was amplified as a 3.2-kb fragment using the primer pair # 1 (Supplementary Table 1); it extended from nucleotide (nt) 6 of exon 1 to nt 77 of exon 2 (numbering based on Ensembl *Pcsk1* locus ID # ENSMUSG00000021587). It was digested at an *Xho*I site, located at nt 252 in the first intron, and at a 3′-most *Bam*HI site created with the PCR primer; the resulting 2.7-kb fragment was cloned into corresponding sites upstream to the *neo* gene for bacterial neomycin phosphotransferase II (NPTII) under the mouse phosphoglycerate kinase 1 (PGK) promoter. The 3′ homology amplicons was obtained using primer pair # 2 (see Table 1). It was 6.6 kb long and extended from nt 34 in exon 10 to nt 460 of exon 13. It was digested at the 5′-most *Sal*I site created with the PCR primer and at a *Kpn*I site located 0.56 kb upstream of intron 12 acceptor splice site. The resulting 3.6-kb 5′ fragment was inserted in the corresponding sites downstream to the *neo* gene and upstream of the Herpes Simplex virus thymidine kinase (*tk*) gene driven by a PGK promoter. The final vector was named pPC1KO.

Table 1
Distorted genotype distribution among offspring of heterozygote intercrosses[a]

Pcsk1 genotype[b]	♀	♂	Total	%[c]
+/+	47	41	88	20
+/−	180	175	355	80
−/−	0	0	0	0

Symbols: ♀, female; ♂, male.
[a] Number of litter: 76; total number of mice: 443.
[b] Genotyping was performed by PCR at weaning.
[c] Expected distribution: 33% +/+ and 67% +/−; $p<0.00001$, χ^2 test.

Production of Pcsk1 mutant mice

From the pPC1KO vector, a 10.4-kb insert, extending from the start of the 5′ homology region to the end of the *tk* gene, was excised by digestion with *Xho*I and *BstE*II and purified. The fragment was used to produce *Pcsk1*$^{+/-}$ (+/−) embryonic stem cells (ES) and mice, as previously described (Zhu et al., 1998). Briefly, the DNA insert was electroporated into R1 embryonic stem (ES) cells; clones resistant to G418 (due *neo* integration) and to Gancyclovir (loss of the *tk* gene) were selected; *Pcsk1* recombinant clones were injected into the inner mass of blastocysts derived from C57BL/6J (B6) mice; the blastocysts were implanted into pseudo-pregnant foster mice; male chimeric offspring were mated with B6 females to generate +/− mice. After backcrossing the mutation into the FVB/N genetic backgrounds for 4 generations, a colony of mutant and wild-type mice was maintained by intercrosses of the incipient congenic heterozygotes. Animal manipulations were approved by the institutional Animal Care Committee; they were performed following the guidelines of the Canadian Council on Animal Care.

Blot analyses

Southern blot analysis was performed as previously described (Mbikay et al., 1997): genomic DNA was extracted from ES cells or mouse tail tips by proteinase K digestion followed by phenol chloroform extraction and ethanol precipitation; it was digested with either *Bam*HI or *Pst*I, fractionated on agarose gel, transferred onto a nylon membrane that was radioactively probed for *Pcsk1*-specific restriction fragments. The probe for *Bam*H1 digests was a 0.66-kb DNA fragment derived from the PC1 promoter; for *Pst*I digests, it was a 0.69-bp fragment derived from intron 14.

Western blot analysis was performed with chemiluminescence revelation as previously described (St. Germain et al., 2005). Primary antibodies consisted of rabbit antibodies against the C-terminus of PC1 (Benjannet et al., 1991, 1993), and mouse monoclonal antibody against β-actin (Cederlane, Mississauga, ON). Semi-quantitative densitometry of immunoreactive bands was conducted on the ChemiGenius Bioimaging System using the Genetools software (Syngene, Frederick, MD).

PCRs

PCR genotyping of the mice was conducted using a 3-primer set # 3 (see Supplementary Table 1), consisting of a forward primer derived from the region near the acceptor site of intron 1 and two reverse primers, one derived from the 3′ end of exon 2 (missing in the disrupted allele) and the other from the 5′ end of the PGKneo gene (missing in the wild-type allele). DNA from tail tip or ear lobe snippets was extracted as previously described (Mbikay et al., 1997). Genotyping of individual embryos was performed using the REDExtract-N-Amp Tissue PCR kit PCR mix as described by the manufacturer (Sigma, St. Louis, MO).

RT–PCR was conducted as follows: total pituitary RNA was reverse-transcribed into cDNA using dT_{18} primer and the Superscript II RNase H$^-$ Reverse Transcriptase (Gibco Life Technologies, Burlington, ON); the cDNA was used as a template to produce PCR amplicons for PC1, PC1pro-pgkneo and PC1pro-neo using primer pairs # 4, #5 and # 6, respectively (see Supplementary Table 1).

Quantitative RT–PCR for the levels of PC1 and TATA box-binding protein (TBP) mRNAs was performed using the *Taq*man technology (Holland et al., 1991). Each reaction mix contained anterior pituitary cDNA as template, 1× FastStart *Taq*Man Probe Master-Rox master mix (Roche, Laval, QC), a specific primer pair and an UPL fluorogenic probes selected from the Roche Universal Probe Library (Supplementary Table 2). The PCR was performed in a Stratagene Mx3005P thermocycler. Standard curves were established using varying amounts of pre-quantified amplicons of each transcript. The level of the TBP mRNA was used for normalization.

Peptide extraction and mass spectrometry analysis

Mouse anterior pituitary peptides/proteins were acid extracted following the protocol of Che et al. (2005). Samples were extracted in 100 µl of 10 mM HCl by sonication three times for 5 s, followed by incubation at 70 °C for 20 min. Extracts were neutralized by addition of 100 µl 0.2 M phosphate buffer, pH 9.5, containing protease inhibitors (Roche Complete Mini Protease Inhibitor Tablets) and centrifuged at 50,000×*g* for 40 min at 4 °C. The pellets were processed as above twice and supernatants combined. Immunoprecipitation of extracted peptides/proteins were carried out in 1× Tris-buffered saline (pH 7.6) containing 0.1% Tween (TBST). Samples were precleared by incubation with preimmune serum in the presence of Protein A-agarose overnight at 4 °C. They were centrifuged at 14,000×*g* for 2 min at 4 °C and supernatants incubated with anti-βEND antibody as above. Following immunocapture, the antibody–antigen complexes were washed five times in TBST and eluted from the Protein-A beads by two successive incubations in 150 µl of 0.1 M glycine (pH 2.8) for 10 min at room temperature with shaking. Supernatants were collected, combined and neutralized with 30 µl of 1 M Tris–HCl (pH 9.0). The eluates were equilibrated in 20% acetonitrile (ACN)/0.1% trifluoroacetic acid (TFA) with an Amicon Ultra YM3 Centricon (Millipore Corp., Bedford, MA), lyophilized and solubilized in 5 µl of 20% ACN+0.1% TFA. For time-of-flight mass spectral analysis, 2.5 µl of each sample were applied twice to a spot on a gold ProteinChip Array (Ciphergen Biosystems Inc, Palo Alto, CA) and allowed to air dry at room temperature after each application; 1 µl of saturated 3,5-dimethoxy-4-hydroxycinnamic acid (SPA) in 50% ACN+0.5% TFA was added to each spot. Mass spectral analysis was performed by time-of-flight mass spectrometry in a Ciphergen Protein Biology System II (PBS II). Analyses represent an average of 100 shots. Masses were calibrated externally with All-in-1 Peptide Standards (Ciphergen Biosystems Inc.). All data were normalized for total ion current and peak areas calculated using the indirect method (with a bracket height of 0.4 and width expansion factor of 2) contained within Ciphergen's ProteinChip Software 3.1.

Embryo culture

Superovulation was induced in female mice by intraperitoneal injection (i.p.) of 5 international units (IU) of pregnant mare serum gonadotropin (PMSG) followed, 48 h later, by 5 IU human chorionic gonadotropin (hCG). The mice were placed with males overnight to mate; mating was ascertained the next day by the presence of a vaginal plug. The mice were sacrificed by cervical dislocation. Eggs and embryos were collected from the oviduct into a drop of KSOM medium (95 mM NaCl, 2.5 mM KCl, 0.35 mM KH_2PO_4, 0.2 mM $MgSO_4{\cdot}7H_2O$, 10 mM Na lactate, 0.2 mM glucose, 0.2 mM Na-pyruvate, 4 mM $NaHCO_3$, 1.7 mM $CaCl_2{\cdot}2H_2O$, 1 mM glutamine, 0.01 mM EDTA, 240 mosM, 0.16 mM K-penicillin G, 0.03 mM streptomycin sulfate) containing 21 mM HEPES and 0.01% polyvinyl alcohol (HEPES/KSOM/PVA) as well as 1 mg/ml hyaluronidase, washed through successive transfer into 1 drop of fresh HEPES–KSOM/PVA and 3 drops KSOM/PVA under mineral oil (Lawitts and Biggers, 1993). They were incubated in the last drop at 37 °C under a 5% CO_2/95% air atmosphere for up to 6 days. Alternatively, unfertilized eggs were collected 24 h post hCG from females that were superovulated but not mated; 1-cell, 2-cell, 6/8-cell, morula and blastocysts were collected from superovulated and mated females, 28, 32, 72, 98 and 120 h post hCG, respectively.

Expression vectors and transfection

The 1.1-kb PC1pro-neo cDNA amplified by RT–PCR from pituitary RNA of *Pcsk1*$^{+/-}$ mice was first subcloned into pCR4TOPO plasmid (Invitrogen, Burlington, ON); it was then excised from this vector with *Spe*I and *Not*I and transferred directionally between *Nhe*I and *Not*I sites into the pCIneo eukaryotic expression vector (Promega, Ottawa, ON), under the human cytomegalovirus promoter–enhancer to generate the pCIneo/PC1pro-neo vector. Similarly, a 7B2-expression vector was made by inserting the full-length cDNA for rat 7B2 between the same two restriction sites.

For transfection, human embryonic kidney HEK293 cells were seeded into 6-well plates at a density of 7.5×10^5 per well in DMEM containing 10% fetal bovine serum (FBS); they were cultured to 75% confluence in a 5% CO_2–95% air atmosphere at 37 °C; they were then transfected in triplicate with 1 µg of a single or mixed vector DNA using Lipofectamine Reagent liposomes as specified by the manufacturer (Life Technologies, Burlington, ON); they were

incubated for 48 h before metabolic labeling with radioactive methionine/cysteine.

Metabolic labeling and immunoprecipitation

Transfected HEK293 cells were rinsed twice with phosphate-buffered saline (PBS), layered with 1 ml/well of methionine and cysteine-free RPMI medium (ICN Biomedicals, Nepean, ON) and incubated at 37 °C for 30 min to deplete endogenous methionine. RPMI medium containing 250 μCi of ^{35}S-methionine–cysteine/ml/well was substituted and incubation was resumed for 2 h. Spent media were collected and cells were scraped off the dishes into 400 μl of RIPA buffer (50 mM Tris–HCl, 1% Nonidet P-40, 0.5% sodium deoxycholate, 150 mM NaCl, 1% SDS). Media and cell lysates were supplemented with 0.04 volumes of a complete protease inhibitor cocktail (Boerhinger Manheim, Laval, QC; 25× stock solution: 1 tablet/2 ml). They were vigorously mixed on a vortex for 2 min, placed on ice for 30 min and centrifuged at 10,000×*g* for 10 min at 4 °C. Supernatants were collected and each was supplemented with 2 μl of normal rabbit serum and 15 μl of a 50% (w/v) suspension of Protein A-agarose. After a 1-h incubation at 4 °C with rotational mixing, the samples were centrifuged at 3000×*g* for 5 min at 4 °C. Supernatants were collected and each was supplemented 5 μl of rabbit anti-7B2 (Paquet et al., 1994) or anti-NPTII antibody (Sigma). They were incubated with mixing as above. The resin with bound immune complexes was then sedimented by centrifugation as above, rinsed three times with RIPA buffer, twice with a buffer containing 1 M NaCl, 10 mM Tris–HCl and 1 mM EDTA, pH 8, and twice with PBS containing 1 mM EDTA. Pellets were suspended in 25 μl of 1× Laemmli buffer each, boiled for 5 min, and sedimented as above. Supernatant was subjected to electrophoresis through polyacrylamide gels (8 or 12%). Gels were fixed for 30 min in a 50% methanol–10% acetic acid solution, treated for 30 min with Amplify fluor solution (Amersham Biosciences, Baie d'Urfé, QC), dried under vacuum and exposed to phosphorimaging screen overnight. Specific radioactive protein bands were visualized and quantified on a Typhoon Phosphorimager (Molecular Dynamics, Sunnyvale, CA).

Feeding, weight and plasma glucose

Four-week-old mice were divided into groups (n=6/gender/genotype) that were fed either a low-fat diet (LFD) or a high-fat diet (HFD) (diets no. D12450 or no D12451, respectively, obtained Research Diet, North Brunswick, NJ); the LFD contained 10% kcal and the HFD 45% kcal as fat. Body weight was recorded weekly. After 13 weeks, the mice were fasted for 16 h, anesthetized with isoflurane (Abbott Laboratories, Montreal, QC) and bled by heart puncture. Some mice were i.p. injected with glucose (1.5 mg/g body weight) and blood collected as above 10 or 60 min later. Plasma was separated from blood cells by centrifugation 600×*g* for 10 min. Plasma glucose was determined using a glucose analyzer (Beckman Coulter, Fullerton, CA).

Statistics

Significance was determined by unpaired Student's *t* test.

Results

Production and analysis of Pcsk1 mutant mouse

The disruption vector is shown in Fig. 1A. Homologous recombination between this vector and the *Pcsk1* locus should result in the excision of 32.7 kb of internal domain including exon 3 to exon 9. The recombination construct was excised

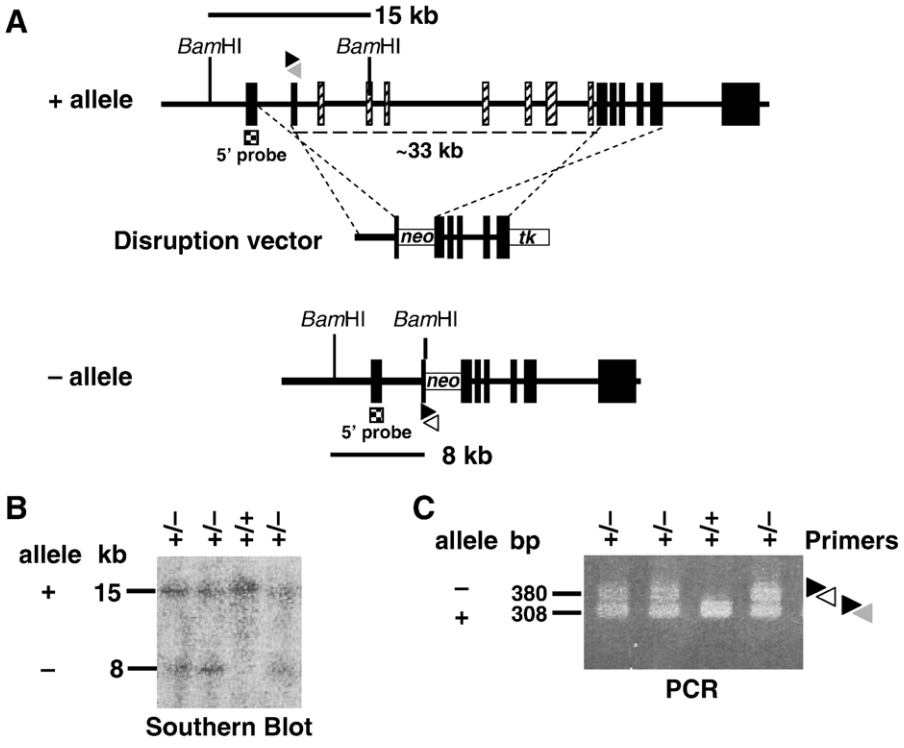

Fig. 1. Production and screening of *Pcsk1* mutant mice. (A) The wild-type allele (+), the disruption vector and the disrupted allele (−) after homologous recombination are diagrammatical depicted. The *Bam*H1 fragments generated detectable by Southern blot analysis is shown above the wild-type allele (15 kb) and below the disrupted allele (8 kb). The 3-primer set # 3 used for PCR genotyping (see Table 1) are represented by arrowheads: the black rightward-pointing arrowhead stands for the 3′ intron 1 forward primer; the white leftward-pointing arrowheads for reverse primers, the white one for the 5′ exon 2 reverse primer and the grey one for the 5′ PGK reverse primer. (B) Southern blot analysis of genomic DNA from offspring of heterozygous intercross using a probe derived from exon 1. The 8 kb and 15 kb bands represent the disrupted (−) and wild-type (+) *Pcsk1* alleles, respectively. (C) Triplex PCR of the same genomic DNA using the 3-primer set # 3.

Table 2
Genotype distribution among preimplantation embryos from heterozygote intercrosses

Embryo st [a]	Total	Number of embryos per *Pcsk1* genotype (%)		
		+/+	+/−	−/−
1-cell	22	8 (36)	7 (32)	7 (32)
2-cell	32	8 (25)	18 (56)	6 (19)
4-cell	20	8 (40)	11 (55)	1 (5)
6- to 8-cell	37	6 (16)	30 (81)	1 (3)
Morula	24	2 (8)	22 (92)	0 (0)
Blastocyst	56	6 (11)	50 (89)	0 (0)
E7.5	37	1 (3)	36 (97)	0 (0)
E15–E16	26	2 (8)	24 (92)	0 (0)

[a] E, embryonic day.

Table 3
Genotype distribution among the offspring of wild-type to heterozygote reciprocal crosses[a]

Parental genotype			*N* [a]	Offspring genotype [b]	
♀	×	♂		+/+ (%)	+/− (%)
+/+	×	+/−	17	35 (40)	52 (60)
+/−	×	+/+	9	16 (33)	33 (67)

[a] Number of litter.
[b] Expected distribution: 1:1, $p<0.01$, χ^2 test.

from the vector and transfected into R1 ES cells; clones were selected for resistance to G418 and Gancyclovir; they were screened by Western blotting for the anticipated *Bam*H1 and *Pst*I, fragments using probes derived from the promoter and from exon 14, respectively (not shown).

Two clones showing the expected restriction fragment patterns were injected into B6 blastocysts; the latter were implanted into foster female mice; male chimeric mice born from these foster mothers were crossed with B6 females to produce offspring that are heterozygous for the *Pcsk1* deletion–insertion (+/−). These were identified either by Southern blotting analysis of *Bam*H1 digests (Fig. 1B) or by triplex PCR (Fig. 1C) of tail-tip genomic DNA.

Homozygote lethality and transmission ratio distortion

When +/− mice were intercrossed, no homozygous *Pcsk1* mutant (−/−) mice were obtained (Table 1). Genotyping of preimplantation embryos derived from these crosses revealed the presence of a significant percentage of −/− embryos at the 1-cell (31%) and 2-cell (19%) stages; this percentage was below 5% at 4-cell and 8-cell stages and 0% at later stages (Table 2), suggesting that lethality occurred after the second embryonic division. Interestingly, the frequency of the mutant allele among surviving late preimplantation (morula to blastocysts), post-implantation and weanlings was consistently ≥80% instead of the 66.7% expected ($p<0.0001$, by χ^2) (Tables 2 and 3), an indication of preferential transmission of this allele. This preference was still observed in +/+×+/− reciprocal crosses (Table 3), excluding any parental origin effect.

To determine whether the lethality of −/− preimplantation embryos was due to intrinsic developmental failure, we cultured fertilized eggs from +/+×+/+ and +/−×+/− crosses and followed their growth for 6 days. We reasoned that death of −/− embryos resulting from heterozygote intercrosses should be reflected by a significant decrease in the number of living embryos at some stage past the second cell division. The results are shown in Fig. 2. Most embryos looked morphologically healthy on day 6 (93%, $n=88$ for +/+×+/+ crosses and 98%, $n=83$ for +/−×+/− crosses, hereafter called mixed embryos). However, the growth pattern were distinct: on day 2, all the fertilized eggs reached the 2-cell stage; but on day 3, 45% of the +/+ embryos and only 22% of mixed embryos reached the morula stage; on day 4, the latter caught up with the +/+ as all became morula; but they grew slightly faster on the 2 subsequent days, with 79% reaching the blastocyst stages (vs. 67% for +/+

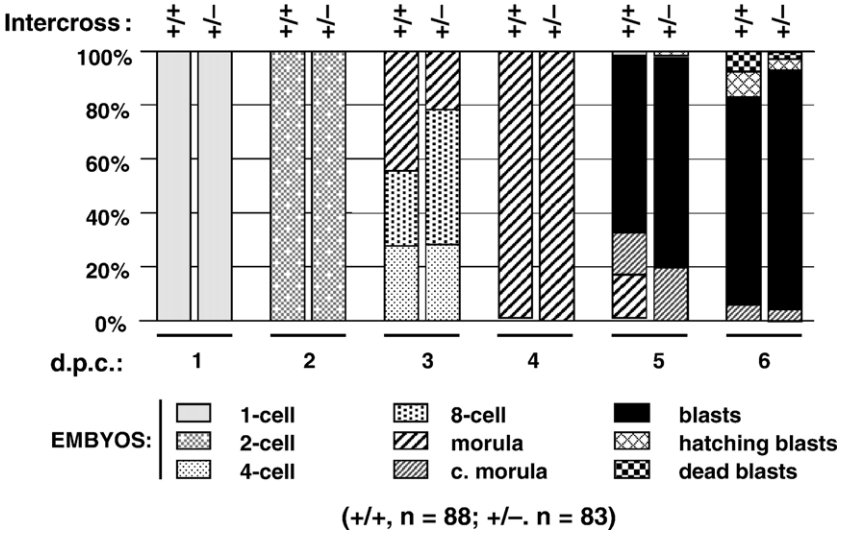

Fig. 2. In vitro development of preimplantation embryos from *Pcsk1*$^{+/+}$ and *Pcsk1*$^{+/-}$ intercrosses. Superovulated female mice were mated to males of the same genotype: +/+×+/+ are labeled as +/+ and +/−×+/− as +/−. Fertilized eggs were collected, cultured and scored on a daily basis for developmental stage. dpc, day post-coitus; c. morula, compacted morula; blasts, blastocysts.

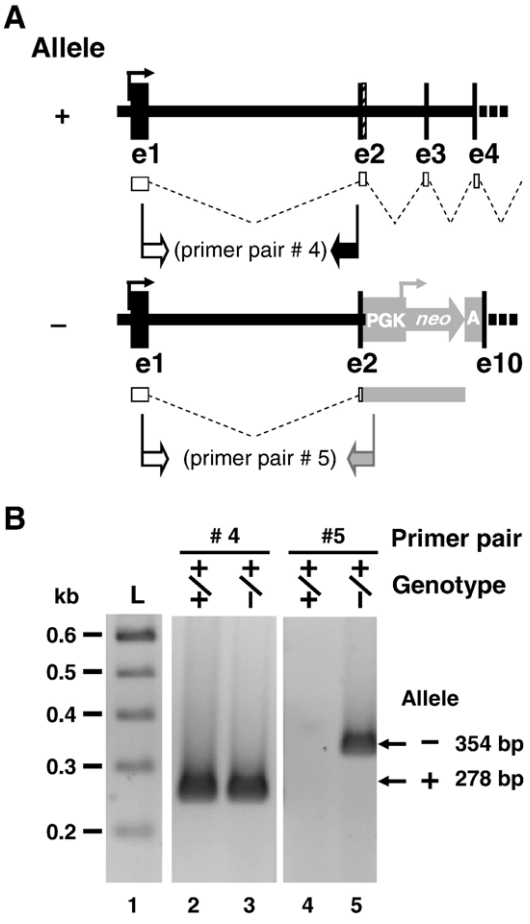

Fig. 3. Identification and characterization of aberrant mRNAs transcribed from the mutant allele. (A) Diagrammatic representation of the 5′ region of the wild-type (+) and disrupted (−) *Pcsk1* allele with below the expected transcript represented below. Intron 1 splicing out is represented with broken lines; primer regions with inverted flags. The prefix "e" in e1, e2 etc stand for exon. (B) Agarose gel analysis of RT–PCR amplicons from pituitary RNA from +/+ and +/− male mice, using primer pairs # 4 and # 5.

embryos), and 94% (vs. 86% for +/+ embryos) on day 5 and day 6, respectively. All three genotypes were detectable by PCR among blastocysts from heterozygote intercrosses. The survival of −/− embryos in culture suggests that their lethality in vivo may be caused by negative selection in the oviductal environment.

Expression of an aberrant PC1neo fusion mRNA

In the mouse model of targeted inactivation of the *Pcsk1* locus reported by Zhu et al. (2002b), the promoter and the first exon were ablated; prenatal and perinatal lethality of homozygous mutants was observed, but nearly 33% of them survived to adulthood. In an attempt to explain the preimplantation lethality of our model, we examined the possibility that the PC1 promoter in the mutant allele could drive the production an aberrant mRNA and protein that could aggravate the phenotype. A potential primary transcript of the mutant locus would include exon 1, intron 1, a 5′ fragment of exon 2 and the PGKneo sequence down to the polyadenylation signal. After removal of intron 1, this transcript should generate an mRNA with open reading frame (ORF) specifying the signal peptide and an N-terminal propeptide segment of PC1 fused to an extension of indeterminate size (Fig. 3A).

To verify whether such an mRNA was produced, we conducted an RT–PCR on pituitary mRNA from +/+ and +/− mice using primer pair # 4 for wild-type PC1 mRNA or primer pair #5 for the putative PC1neo fusion mRNA. The pituitary was selected as source of RNA because it expresses high levels of PC1 (Seidah et al., 1990, 1994), a reflection of PC1 gene promoter activity. Polyadenylated RNA was specifically reverse-transcribed into cDNA using an oligo-dT primer. The RT–PCR results are shown in Fig. 3B. With primer pair #4, the expected amplicon of 278 bp was detected in both samples (lanes 2 and 3). In contrast, using primer pair #5, the expected amplicon of 354 bp was obtained from +/− pituitaries (lane 5), but not from +/+ pituitaries (lane 4), confirming the existence of the aberrant mRNA. This mRNA was also detectable in pools of unfertilized eggs, fertilized eggs and preimplantation embryos obtained from +/− intercrosses (not shown).

To establish the full sequence of these transcripts, oligo-dT-primed cDNA from +/− mouse pituitary RNA was subjected to long-range PCR using a forward primer derived from the region upstream to the initiator ATG in PC1 exon 1 and a reverse primer from the neo mRNA 3′-UTR (primer pair #6). Three cDNA amplicons of 1.6, 1.4 and 1.1 were obtained and sequenced (Fig. 4A). They corresponded to alternate splice variants of the primary transcript. The predictability of the splice sites were confirmed a posteriori using the NNSPLICE 0.9 version algorithm (Reese et al., 1997) online (http://www.fruitfly.org/seq_tools/splice.html). The 1.6-kb and 1.4 amplicons encoded a fusion protein made of the 27-amino acid (aa) signal peptide and the first 58 aa of the propeptide of PC1 followed by a 48-aa extension encoded by the PGK sequence (not shown). The 1.1 amplicons specified a single ORF consisting of the same 85-aa PC1 prepropeptide fused to the full NPTII sequence by a 12-aa joining peptide (Fig. 4B). This amplicon was cloned into the PCIneo expression vector and the resulting vector was transiently transfected into HEK293 cells. Metabolic labeling followed by NPTII-specific immunoprecipitation and SDS–PAGE revealed the presence of the PC1pro-NPTII (~37 kDa) and a processed NPTII (~27 kDa) in cell extracts and media (Fig. 4C, lanes 2 and 4). The size of secreted NPTII was smaller than predicted for NPTII (~32 kDa) if the propeptide was the only segment removed, suggesting that the mature protein underwent other forms of proteolytic processing in the secretory pathway. A 68-kDa protein was co-immunoprecipitated with the NPTII-related proteins from cells expressing the fusion protein (lane 2); its identity is unknown.

Inhibitory activity of aberrant mRNA translational products

The precursor for the neuroendocrine protein 7B2 is a model substrate for testing proprotein convertase activity ex vivo.

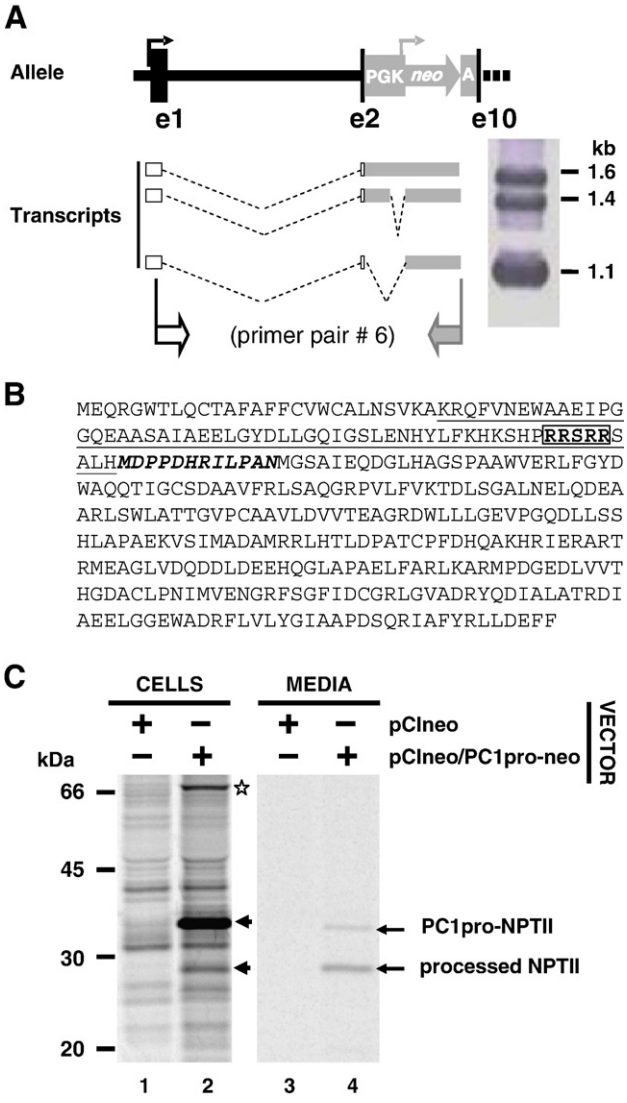

Fig. 4. Full-length aberrant mRNAs from the mutant allele. (A) Diagrammatic representation of the 5′ region of the disrupted *Pcsk1* allele. RNA was extracted from the pituitary of +/− male mice and subjected to long-range RT–PCR using primer pair # 6 are shown. Agarose gel pattern of the resulting amplicons is below at the right of their diagrammatical representation. Splicing events deduced from the sequence of the transcripts are represented with broken lines; and primer regions with inverted flags. The prefix "e" in e1, e2, etc., stands for exon. (B) Amino acid sequence of the protein specified by the 1.1 cDNA amplicon: the PC1 sequence includes the signal peptide and the first half of the propeptide (underlined); it is followed by a joining peptide (bold and italics), and the NPTII sequence. The furin recognition site in the propeptide region is bolded and boxed. (C) Expression and processing of PC1prepro-NPTII in transfected HEK293 cells. Cells transfected with the specified expression vector were metabolically labeled with ^{35}S-methionine and NPTII proteins analyzed by immunoprecipitation and SDS–PAGE. Proteins derived from the PC1prepro-NPTII are identified with arrowheads (cells) and arrows (medium). An intracellular protein that co-immunoprecipitates with the fusion protein is indicated with a star.

Transduced into cells, it can be cleaved by most PCs after one or more of the paired basic residues located in the C-terminal region, generating a pattern of processed products that differ among cell lines (Benjannet et al., 1997). The expected fragments are diagrammatically represented in Fig. 5A.

To determine whether the PC1pro-NPTII could affect pro7B2 processing, we transiently co-transfected expression vectors for this aberrant protein and for pro7B2 into HEK293 cells. These cells express furin, PACE4, PC5 and PC7 (Tsuji et al., 2002). The cells were metabolically labeled and 7B2-related proteins were identified following immunoprecipitation, SDS–PAGE and phosphorimaging. 7B2-immunoreactive proteins of estimated molecular weights of 30, 28, 25 and 23 kDa were observed (Fig. 5B); they presumably correspond to $7B2^{1-186}$, $7B2^{1-171}$, $7B2^{1-161}$ and $7B2^{1-150}$, respectively (see Fig. 5A). $7B2^{1-161}$ and $7B2^{1-150}$ are the major secreted forms. The relative abundance of each 7B2 form (% of total) is shown in Fig. 5C. Of all the forms, only the 28-kDa $7B2^{1-171}$ form was significantly reduced in the presence PC1pro-NTPII. PC5A has been shown to generate this form when co-expressed with pro7B2 in monkey kidney BSC40 cells (Benjannet et al., 1997). These results support the possibility that, in +/− early embryos, aberrant products from the *Pcsk1* mutant allele could reduce proteolytic activation of precursors to functional proteins or peptides by broader inhibition of proprotein convertases activities.

Reduced PC1 expression in the anterior pituitary of $Pcsk1^{+/-}$ mice

PC1 expression in the anterior lobe of the pituitary of +/+ and +/− mice was compared at the mRNA and protein levels. We chose this lobe because it is the primary site of PC1 expression in this organ (Seidah et al., 1990). Quantitative RT–PCR analysis was conducted using a primer pair that will amplify transcripts from the wild-type *Pcsk1* allele only. The anterior pituitary content of PC1 mRNA was comparable between genotypes and between genders. There was a trend towards greater PC1 mRNA levels expression in males than in females of the same genotype (Fig. 6A).

A semi-quantitative immunoblotting of anterior pituitary extracts from +/+ and +/− male mice was conducted using an antibody against a C-terminal fragment of PC1 (identified in Fig. 6B-a). In both genotypes, this antibody recognized a ~80-kDa and a ~20-kDa forms, presumably representing mature $PC1^{1-643}$ and the C-terminal peptide PC1-$CT^{509-643}$ (Fig. 6B-b). However, the two PC1 fragments were significantly less abundant in anterior pituitary extracts from +/− mice ($p<0.01$, $n=4$) (Figs. 6B-b and c).

Using mass spectrometry (MS), we analyzed the relative abundance of POMC-derived peptides immunoprecipitated with the anti-βEND antibody from acid extracts of anterior pituitaries from males and female mice of both genotypes. Representative MS profiles of these peptides are shown in Fig. 7A. The identities of the peptides specifically immunoprecipitated are provided in Fig. 7B. The identification was based on the close proximity between the expected and the observed molecular masses of the peptides (Supplementary Fig. 1). The MS profiles significantly differed between male and female mice, with males producing more βEND and less βLPH than females. However, within each gender, there was no significant difference between +/+ and +/− mice (Fig. 7C).

Effect of dietary fat on weight gain in wild-type and mutant mice

Genetic PC1 deficiency in human causes congenital obesity (Jackson et al., 1997). A similar phenotype was observed in the recently reported *Pcsk1*$^{N222D/N222D}$ mouse (Lloyd et al., 2006). In the mouse model lacking the promoter and exon 1 of the *Pcsk1* gene (Zhu et al., 2002b), it leads to reduced body mass and weight gain with age, relative to +/+ mice, but causes a trend towards greater weight gain in +/− mice. In our model, no significant difference in these parameters was observed between the two genotypes when mice were fed normal chow (not shown). However, when the effect of low-fat diet (LFD) or high-fat diet (HFD) on weight gain with age was examined, some differences were noted (Fig. 8, $n=6$ per group). At 4 weeks of age, mice of the same gender were of comparable weight, irrespective of the genotype (26.5±1.1 g for +/+ vs. 27.1±1.0 g for +/− males; 21.0±0.4 g for +/+ vs. 21.0±0.9 g for +/− females). After 13 weeks of LFD, male mice of both genotypes gained comparable amount of weight (23% for +/+ mice vs. +25% for +/− mice); but +/− female mice gained significantly less (9%) weight than their +/+ counterparts (26%). After 13 weeks of HFD, male mice of both genotypes gained more weight than those under LFD (40% vs. 23% for +/+ mice; 33% vs. 25% for +/− mice). In contrast, female mice responded differently to the increase in dietary fat intake: whereas +/+ were insensitive to it, gaining the same amount of weight (23%) under either diet, +/− mice, on the other hand, were highly sensitive to it, gaining 43% more weight under HFD compared to 9% more under LFD. Plots of weights with increasing age under the two diets per gender and per genotypes are provided as Supplementary Fig. 3. These results suggested that the mutation at the *Pcsk1* locus affected female body response to dietary fat content.

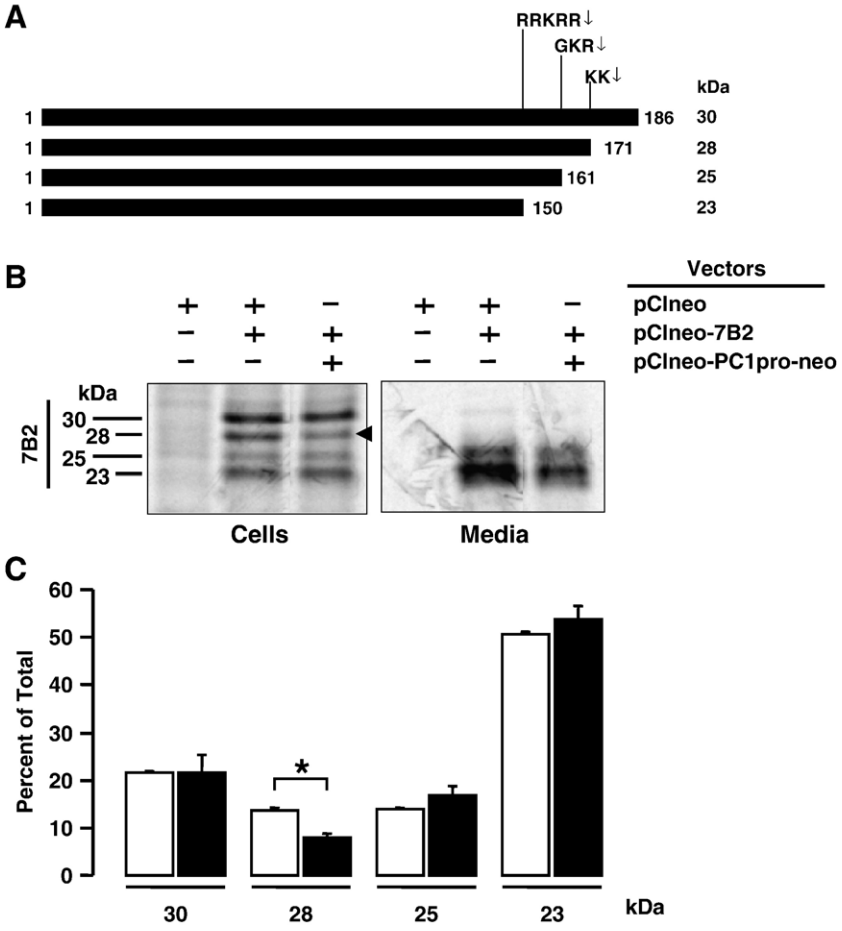

Fig. 5. Inhibition of pro7B2 processing by PC1pro-NPTII. (A) Diagrammatic representation of pro7B2 (top bar) and of known products of its processing by PCs (lower bars). The basic residues preceding the cleavage sites are given on top of the top bar. The number of the first and last residue of each form is indicated at the start and the end of each bar, respectively, taking into account carboxypeptidase (CP)-mediated removal of terminal basic residues after PC cleavage, and amide conversion of the terminal Gly followed CP action. The apparent molecular masses of these forms are given at the right under kDa. (B) Cells were transfected with 1 μg of DNA of pCIneo vector or a mixture of equal amounts of pCIneo and pCIneo-7B2 or of pCIneo-7B2 and pCIneo-PC1pro-neo; 48 h later, they were metabolically labeled with ^{35}S-methionine/cysteine. Cell extracts and spent media were analyzed for 7B2 forms by immunoprecipitation and SDS–PAGE and semi-quantitative phosphorimaging. The 7B2$^{1-171}$ processed form affected by PC1pro-NPTII expression is identified with an arrowhead. (C) Histogram representation of the relative abundance of 7B2 forms in the absence (open boxes) or in the presence (filled boxes) of PC1pro-NPTII. Box heights and error bars represent mean percentages of 7B2 forms and standard errors of these means (SEM), respectively. The experiment was conducted in triplicate. *$p<0.01$.

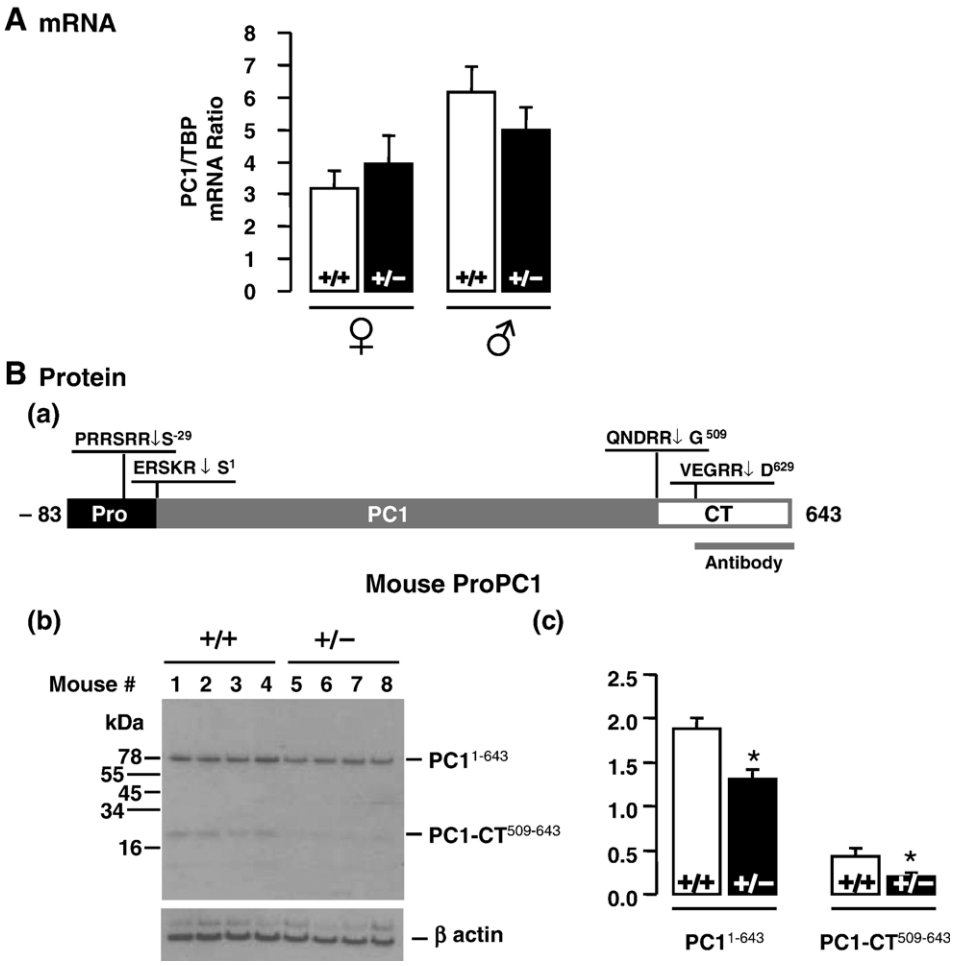

Fig. 6. PC1 expression in anterior pituitaries from individual +/+ and +/− mice. (A) The levels of mRNA for PC1 and TBP were determined by *Taq*man qRT–PCR using primer pairs and fluorogenic probes described in Supplementary Table 2. The forward and reverse primers for PC1 were derived from exon 6 and exon 7, respectively. They should amplify transcripts from the wild-type allele only since the recognized region was ablated in the disrupted allele. The relative levels of PC1 mRNA were derived after normalization for the levels of TBP mRNA. Values represent means of PC1/TBP ratios ± SEM. There was no significant difference between same-gender +/+ and +/− mice. Among +/+ mice, however, ♂ mice contained significantly more PC1 mRNA in their anterior pituitary than ♀ mice ($n=6$). (B) (a) Diagrammatic representation of PC1 domains. The protein is represented as horizontal box, with the prodomain (pro), the fully mature enzyme (PC1) and the C-terminal domain (CT) differentially colored. The P4–P1′ amino acid sequences encompassing the cleavage sites (↓) are shown above the box. The position of the CT antigen used for raise the antibody used in this analysis is shown as a line below the box. (b) Western blot analysis of proteins extracted from anterior pituitaries of individual male mice. Samples were fractionated by 10–20% SDS–PAGE. Membranes were probed with the anti-PC1-CT (upper panel), or an anti-β actin (lower panel) antibody. (c) Comparison of levels of PC1 and PC1-CT peptide. Densities of immunoreactive PC1 bands in (b) were normalized for the cognate densities of the β actin bands. Values represent means of PC1/TBP ratios ± SEM ($n=4$). Compared to +/+ mice, +/− mice contained in 31% and 54% less anterior pituitary PC1 and PC-CT peptide, respectively (*$p<0.01$).

There were no statistical differences between +/+ and +/− mice ($n=4$/gender/genotype) in fasting glycemia (g/l) after 13 weeks of LFD (98.3 ± 18.6 vs. 92 ± 17.5 for males and 98.3 ± 18.6 vs. 92 ± 17.5 for females) and HFD (124 ± 11.9 vs. 103 ± 21.7 for males and 98.3 ± 18.6 vs. 92 ± 17.5 for females) as well as in glycemic response to intraperitoneal glucose injection (not shown), suggesting that the mutation did not induce any significant disturbance of glucose homeostasis.

Discussion

In this report, we have described a mouse model of targeted inactivation of the *PC1* gene by a deletion/insertion. The deletion was about 32.7-kb long; it removed about three quarters of the structural gene, from exon 2 to exon 10. The insertion was a 1.8-kb PGKneo gene. This deletion/insertion caused a complex phenotype consisting of preimplantation lethality of homozygous mutants, preferential transmission of the mutant allele and susceptibility of heterozygous female mice to dietary fat content. We examined the possibility that the disrupted *Pcsk1* region contained any nested genes (Yu et al., 2005) or regulatory mRNAs (Alvarez-Garcia and Miska, 2005), the loss of which might be invoked to explain this phenotype. Analysis of the deleted genomic region using the GeneComber algorithm (http://www.bioinformatics.ubc.ca) revealed two short nested genes specifying peptides with no significant homology with any known protein. A TargetScan search (http://www.targetscan.org) also failed to identify any potential microRNA sequence or target in the disrupted region.

Preimplantation lethality of homozygote mutant embryos was observed among N4 incipient congenic mice of either FVB/N or B6 genetic background. Its causes are still uncertain. Homozygote preimplantation lethality in mouse has generally been associated with intrinsic defects, caused by spontaneous or induced genetic lesions. One example of spontaneous lesions is the lethal yellow (A^y) mutation, a 170-kb deletion at the mouse *agouti* (*a*) locus on Chr 2 (Rinchik et al., 1993). Examples of induced lesions include knockout mice for the mixed lineage leukemia (*MLL*) gene whose product regulates *Hox* gene expression (Ayton et al., 2001), for the xeroderma pigmentosum-associated genes such as the *XPD* gene (de Boer et al., 1998) and the *XAB2* gene (Yonemasu et al., 2005). In some of these genetic lesions, gene ablation was associated with expression of aberrant transcripts that may have contributed to the lethal phenotype. In the A^y mutant mouse, for example, the deletion ablates the structural gene for *Raly*, placing the *agouti* gene under the *Raly* gene promoter and causing ubiquitous expression of this normally neonatal skin-restricted gene. The *Raly* gene specifies an RNA binding protein critical for early growth. Thus, the A^y phenotype results from both *Raly* gene ablation and ectopic expression of the *agouti* gene (Duhl et al.,

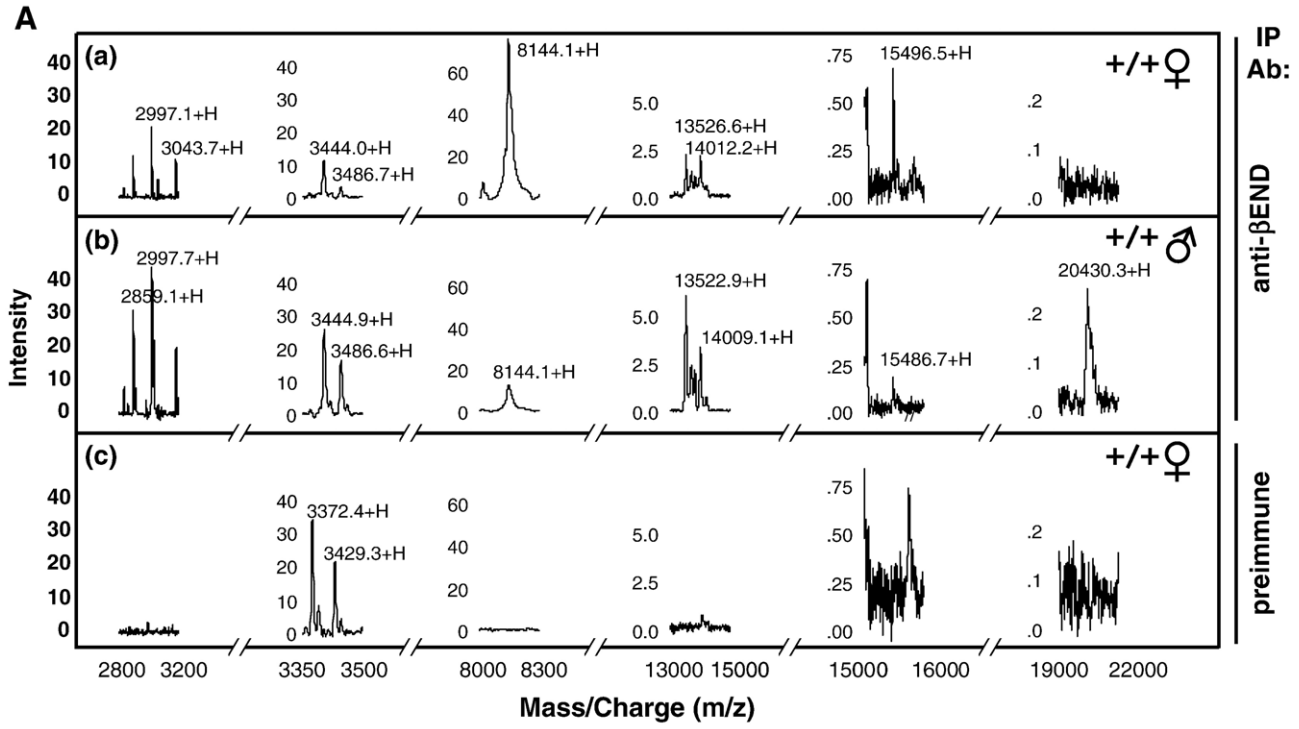

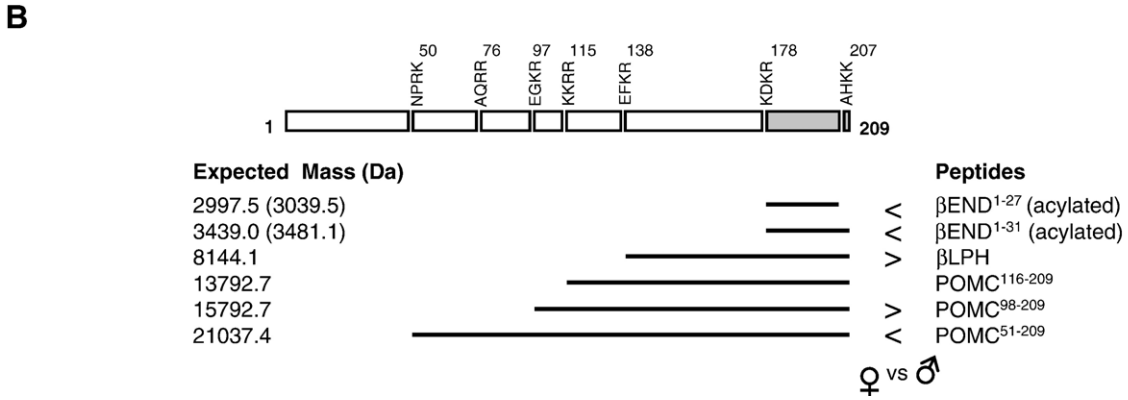

Fig. 7. Mass spectrometry of POMC-derived peptides from the anterior pituitary of +/+ and +/− mice. Peptides were immunoprecipitated (IP) with anti-βEND antibody (Ab) from acid extracts of individual anterior pituitaries from ♀ and ♂ mice. (A) Typical profiles of time-of-flight mass spectral analyses of the molecular masses of the βEND-specific immunoreactive peptides [(a) and (b)] from ♀ (a) and ♂ (b) mice or non-specific peptides immunoprecipitated by a preimmune serum from ♀+/+ mice (c). (B) Schematic representation of major POMC-derived peptides. POMC is represented as a succession of horizontal boxes. Above the bar are provided the P4–P1 tetrapeptide ending with a pair of basic residues. The numbers of P1 residues are indicated. Detected processed peptides are represented as lines below the boxes. Their identities and their expected masses are specified at the right and the left, respectively. Peptides more or less abundant in ♀ than in ♂ mice are flanked by the > or < symbol, respectively. (C) Levels of peptides in each sample were calculated relative to the total ion current and peak areas set as 100%. They are presented mean percentages ± SEM. The number of mice (*n*) used was 7 for ♀+/+ and ♂+/− mice; 6 for ♀+/− female and ♂+/+ mice). Significant differences between ♂ and ♀ mice are indicated in the upper panel as $*p<0.5$, $**p<0.005$ or $***p<0.0005$.

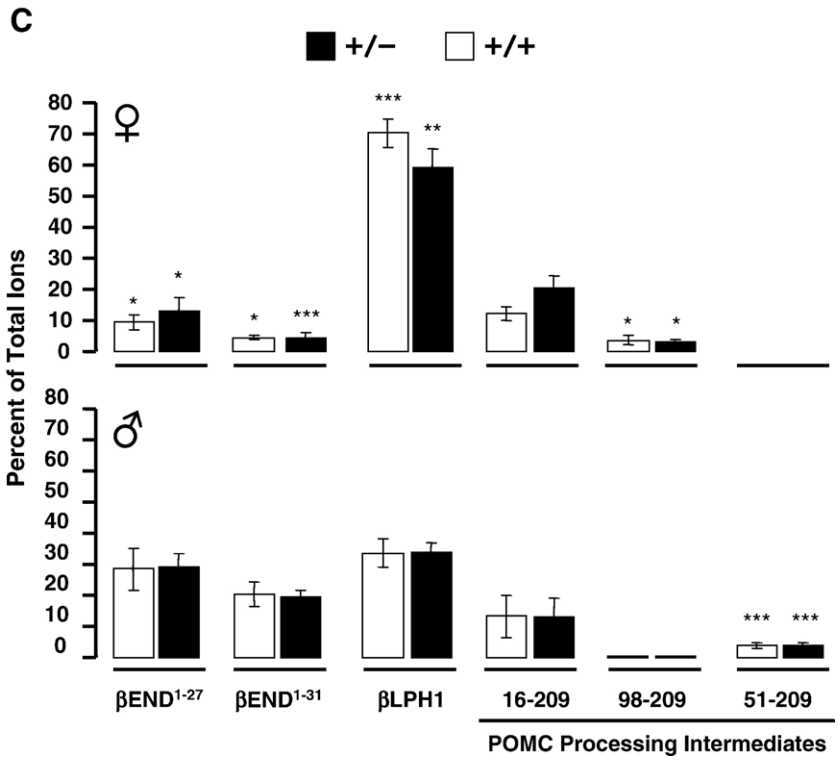

Fig. 7 (*continued*).

1994; Michaud et al., 1993; Yonemasu et al., 2005). In the *MLL*-null mice, the mutant allele expresses truncated in-frame *Mll* transcripts which encode functional domains of the protein (Ayton et al., 2001).

The *Pcsk1* mutation described in this study also causes both gross genetic alterations and production of aberrant transcripts. However, it is unlikely that these structural and expression abnormalities in the mutant allele are the sole determinants of the preimplantation lethality of −/− embryos in vivo, since nearly all fertilized eggs from heterozygote intercrosses can develop to the blastocyst stage in vitro (Fig. 2). The growth pattern of these embryos in culture revealed a transient growth delay from the 4-cell to the morula stage, suggesting that this could be the stage of greater vulnerability for the −/− embryos. This is partially supported by the genotyping results of in vivo-grown embryos which show a sharp drop in the frequency of −/− embryos after the second cell division (Table 3). The lethality of these embryos in vivo may be due to a deficiency for autocrine factors needed to survive under the selective environment of the oviduct. This deficiency may be relieved in vitro through factor sharing among embryos. It is known that low-density culture of mouse fertilized eggs impairs their development to the blastocyst stage. This impairment can be partially corrected by supplementation of bioactive peptide such as epidermal growth factor (EGF), transforming growth factor (TGF) α or β1 or platelet-activating factor (O'Neill, 1998; Paria and Dey, 1990).

We have recently shown that transcripts for all PCs, except PC2, are found in fertilized eggs. Expression of PC1, furin, PACE4 and PC7 is maintained during development to the blastocyst stage, while that for PC4 and PC5 gradually subsides (St. Germain et al., 2005). These enzymes may be involved in the proteolytic activation of a number of precursors to autocrine factors and their receptors. The embryo and the oviduct produce several factors through this process, among them, GnRH (Casan et al., 1999, 2000; Kawamura et al., 2005; Raga et al., 1999), IGF-1 and-2, IGF-1 receptor (IGF-1R) and TGFβ1–3 (Dalton et al., 1994; Doherty et al., 1994; Lighten et al., 1997). GnRH and IGF-1 have been shown to act as anti-apoptotic agents on embryos in culture (Fabian et al., 2004; Jousan and Hansen, 2004; Kawamura et al., 2005).

PC1 deficiency in the mutant embryos will undoubtedly lead to impaired processing of precursors to some of these factors. However, considering the overlap in cleavage specificity among PCs (Seidah and Chretien, 1999; Steiner, 1998), furin, PC7 and PACE4 which are expressed throughout preimplantation embryonic development (St. Germain et al., 2005), should be able to partially compensate for this deficiency. The fact that −/− preimplantation embryos survive in the mouse model generated by Zhu et al. (2002b) would support such a view. We speculate that, in our model, the deficit of autocrine factors may be aggravated by a more generalized inhibition of PCs caused by secretory truncated PC1 propeptides produced in −/− embryos. Propeptides derived from the prodomain of PC1 have been shown to inhibit not only PC1, but also furin, PC5 and PC7 (Basak and Lazure, 2003; Boudreault et al., 1998; Fugere et al., 2002). It is interesting to note that embryonic lethality of −/− became noticeable after the 4-cell stage, when degradation of egg-derived mRNAs is virtually complete and activation of the zygotic genome has been initiated (Wang and Dey, 2006). At this

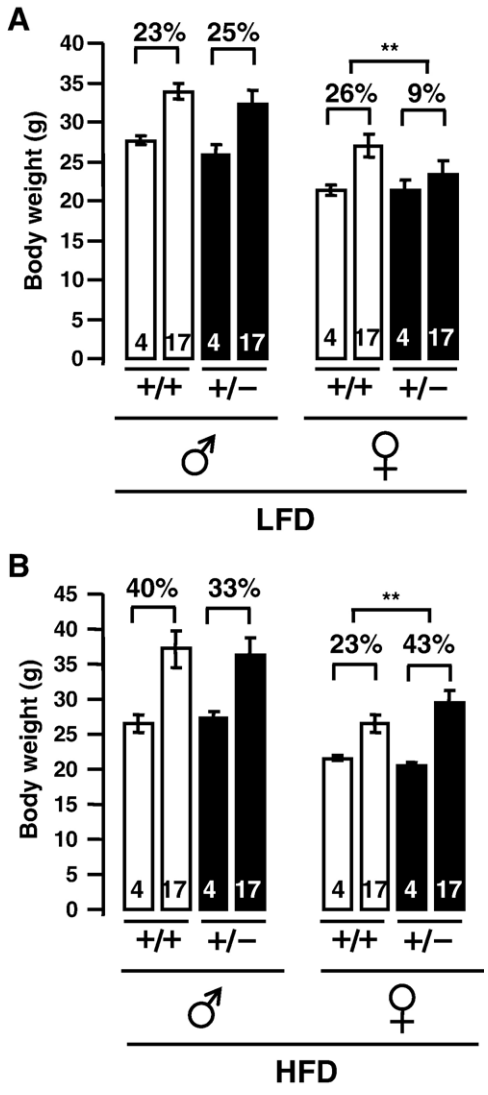

Fig. 8. Effect of dietary fat on age-related weight gain. From 4 to 17 weeks of age, ♂ and ♀, wild-type (+/+, white bars) and mutant (+/−, black bars) mice (n=6/genotype/gender) were fed either a low fat diet (LFD) or a high fat (HFD); they were weighed on a weekly basis. The results are presented histographically as mean body weights (g)±SEM. Mouse ages in weeks at the start and the end of the protocol are indicated within the histographic boxes. The % weight gains at the end of the protocol are indicated .above each box. Significant differences in weight gain between +/+ and +/− mice are indicated above the corresponding boxes as **p<0.001.

stage, activation of both parental mutant alleles would lead to the production and accumulation of the PC1 propeptide fusion proteins with broad inhibitory activity against PCs. This *Pcsk1*$^{-/-}$ mouse may therefore represent a model of multiple convertase deficiency. The model suggests that drug-mediated broad inhibition of PCs could cause early arrest of pre-implantation embryo development.

Another striking feature of this model is the non-Mendelian, higher frequency of the mutant allele among offspring of all cross combinations. The transmission ratio distortion (TDR) became detectable at the 6- to 8-cell stage of embryonic development and persisted to birth. One of the most examined cases of transmission ratio distortion (TDR) in mouse is the *t*-complex inversion on Chr 17. In this mouse, the mutant allele is transmitted to up to 95% of the offspring of t/+ males to +/+ female crosses, due to damaging effect of gene products from the *t*-complex on + sperm during meiosis (Lyon, 2003). Another well-documented case of TDR in mouse is associated with the *Om* mutation on Chr 11. In this case, TDR was observed in the offspring of reciprocal backcrosses of (B6×DDK)F_1 to either parental strain, with preferential transmission of the DDK *Om* allele when F_1 females were mated to B6 males. The distortion has been attributed to meiotic drive leading to preferential segregation of the wild-type chromatids to the polar body during the second meiotic division, leaving the mutant chromatids to contribute to the zygote genome (Wu et al., 2005). The TDR observed with our *Pcsk1*$^{+/-}$ mouse model cannot be explained through either of these meiotic events since it was absent at the 2-cell stage. It is unclear at present whether the distortion is due to a greater survival of +/− embryos or a greater lethality of +/+ embryos, under the selective pressure of the oviductal environment.

In humans, total PC1 deficiency is associated with increased body mass at birth (Jackson et al., 1997). The opposite is observed in PC1-null mice generated by Zhu et al. (2002b). In this mouse model, however, +/− mice gained more weight with age than +/+ mice. In another mouse model of partial PC1 deficiency, a homozygous phenotype of obesity and hyperphagia was reported (Lloyd et al., 2006). In our model, there was no difference between +/+ and +/− mice of the same gender in weaning weight or age-related weight gain under normal chow. The difference between the three models could be due to differences in genetic backgrounds as well as in the nature of the mutations. The influence of genetic background on the morbid phenotype was illustrated in a comparative study of mice carrying a targeted inactivation mutation in the *Pcsk2* and *Sgne1* genes, specifying PC2 and its helper protein 7B2, respectively: both mutations lead to a Cushing-like syndrome in the 129Sv genetic background, but not the B6 one (Peinado et al., 2005).

In the mouse model of PC1 deficiency described in this study, age-induced weight gain is susceptible to dietary fat in female mice: compared to +/+ mice, −/− mice experienced stunted growth under a LFD and catch up growth under HFD. This differential response dietary fat cannot be attributed to differences in appetite since there was no significant difference in food intake between genotypes when mice were fed either a low-fat or a high-fat diet (Supplementary Fig. 3). It was not observed among male mice. The physiological basis for the phenotypic gender dichotomy is unclear. We have observed that the profiles of anterior pituitary POMC-derived peptides were consistently different between male and female mice (Fig. 7). Although these profiles were similar between +/+ and +/− in this tissue, it remains possible that other precursors in other tissues might be differentially processed. The weak inhibitory activity of the aberrant proteins on PC1-mediated processing of pro7B2 in transfected cells (Fig. 5) is not a compelling argument for an in vivo effect. The putative toxicity of these proteins in early development may be unrelated to this activity. Alternatively, it may be due to derangement of macromolecule

interactions and dynamics. To explain the greater susceptibility to PC1-deficient female mice to dietary fat, it will be necessary to examine whether the normal levels of PC1 enzymatic activity differs between genders and whether this is associated with differences in PC1-mediated production of central and peripheral peptide hormones and neuropeptides that control nutrient absorption and metabolism.

In summary, we have described a mouse model of heritable PC1 deficiency caused by a deletion/insertion at the *Pcsk1* locus and associated with homozygote preimplantation lethality, preferential transmission of the mutant allele and female heterozygote susceptibility to dietary fat.

Acknowledgments

The authors are indebted to Mrs. Adrianna Gambarotta, Josée Hamelin, Haidy Tadros, Jennifer Hazelwood and Mr. Andrew Chen for their technical assistance. This work was supported by grants from the Canadian Institute for Health Research.

Appendix A. Supplementary data

Supplementary data associated with this article can be found, in the online version, at doi:10.1016/j.ydbio.2007.03.523.

References

Alvarez-Garcia, I., Miska, E.A., 2005. MicroRNA functions in animal development and human disease. Development 132, 4653–4662.

Anderson, E.D., Molloy, S.S., Jean, F., Fei, H., Shimamura, S., Thomas, G., 2002. The ordered and compartment-specific autoproteolytic removal of the furin intramolecular chaperone is required for enzyme activation. J. Biol. Chem. 277, 12879–12890.

Ayton, P., Sneddon, S.F., Palmer, D.B., Rosewell, I.R., Owen, M.J., Young, B., Presley, R., Subramanian, V., 2001. Truncation of the *Mll* gene in exon 5 by gene targeting leads to early preimplantation lethality of homozygous embryos. Genesis 30, 201–212.

Basak, A., Lazure, C., 2003. Synthetic peptides derived from the prosegments of proprotein convertase 1/3 and furin are potent inhibitors of both enzymes. Biochem. J. 373, 231–239.

Basak, A., Koch, P., Dupelle, M., Fricker, L.D., Devi, L.A., Chretien, M., Seidah, N.G., 2001. Inhibitory specificity and potency of proSAAS-derived peptides toward proprotein convertase 1. J. Biol. Chem. 276, 32720–32728.

Benjannet, S., Rondeau, N., Day, R., Chrétien, M., Seidah, N.G., 1991. PC1 and PC2 are proprotein convertases capable of cleaving proopiomelanocortin at distinct pairs of basic residues. Proc. Natl. Acad. Sci. U. S. A. 88, 3564–3568.

Benjannet, S., Rondeau, N., Paquet, L., Boudreault, A., Lazure, C., Chrétien, M., Seidah, N.G., 1993. Comparative biosynthesis, covalent post-translational modifications and efficiency of prosegment cleavage of the prohormone convertases PC1 and PC2: glycosylation, sulphation and identification of the intracellular site of prosegment cleavage of PC1 and PC2. Biochem. J. 294, 735–743.

Benjannet, S., Savaria, D., Chrétien, M., Seidah, N.G., 1995. 7B2 is a specific intracellular binding protein of the prohormone convertase PC2. J. Neurochem. 64, 2303–2311.

Benjannet, S., Savaria, D., Laslop, A., Munzer, J.S., Chrétien, M., Marcinkiewicz, M., Seidah, N.G., 1997. Alpha1-antitrypsin Portland inhibits processing of precursors mediated by proprotein convertases primarily within the constitutive secretory pathway. J. Biol. Chem. 272, 26210–26218.

Boudreault, A., Gauthier, D., Lazure, C., 1998. Proprotein convertase PC1/3-related peptides are potent slow tight-binding inhibitors of murine PC1/3 and Hfurin. J. Biol. Chem. 273, 31574–31580.

Braks, J.A., Martens, G.J., 1994. 7B2 is a neuroendocrine chaperone that transiently interacts with prohormone convertase PC2 in the secretory pathway. Cell 78, 263–273.

Casan, E.M., Raga, F., Polan, M.L., 1999. GnRH mRNA and protein expression in human preimplantation embryos. Mol. Hum. Reprod. 5, 234–239.

Casan, E.M., Raga, F., Bonilla-Musoles, F., Polan, M.L., 2000. Human oviductal gonadotropin-releasing hormone: possible implications in fertilization, early embryonic development, and implantation. J. Clin. Endocrinol. Metab. 85, 1377–1381.

Che, F.Y., Lim, J., Pan, H., Biswas, R., Fricker, L.D., 2005. Quantitative neuropeptidomics of microwave-irradiated mouse brain and pituitary. Mol. Cell. Proteomics 4, 1391–1405.

Chrétien, M., Seidah, N.G., 1981. Chemistry and biosynthesis of pro-opiomelanocortin. ACTH, MSH's, endorphins and their related peptides. Mol. Cell. Biochem. 34, 101–127.

Dalton, T., Kover, K., Dey, S.K., Andrews, G.K., 1994. Analysis of the expression of growth factor, interleukin-1, and lactoferrin genes and the distribution of inflammatory leukocytes in the preimplantation mouse oviduct. Biol. Reprod. 51, 597–606.

de Boer, J., Donker, I., de Wit, J., Hoeijmakers, J.H., Weeda, G., 1998. Disruption of the mouse xeroderma pigmentosum group D DNA repair/basal transcription gene results in preimplantation lethality. Cancer Res. 58, 89–94.

Dey, A., Norrbom, C., Zhu, X., Stein, J., Zhang, C., Ueda, K., Steiner, D.F., 2004. Furin and prohormone convertase 1/3 are major convertases in the processing of mouse pro-growth hormone-releasing hormone. Endocrinology 145, 1961–1971.

Doherty, A.S., Temeles, G.L., Schultz, R.M., 1994. Temporal pattern of IGF-I expression during mouse preimplantation embryogenesis. Mol. Reprod. Dev. 37, 21–26.

Duhl, D.M., Stevens, M.E., Vrieling, H., Saxon, P.J., Miller, M.W., Epstein, C.J., Barsh, G.S., 1994. Pleiotropic effects of the mouse lethal yellow (A^y) mutation explained by deletion of a maternally expressed gene and the simultaneous production of *agouti* fusion RNAs. Development 120, 1695–1708.

Fabian, D., Il'kova, G., Rehak, P., Czikkova, S., Baran, V., Koppel, J., 2004. Inhibitory effect of IGF-I on induced apoptosis in mouse preimplantation embryos cultured in vitro. Theriogenology 61, 745–755.

Fricker, L.D., McKinzie, A.A., Sun, J., Curran, E., Qian, Y., Yan, L., Patterson, S.D., Courchesne, P.L., Richards, B., Levin, N., Mzhavia, N., Devi, L.A., Douglass, J., 2000. Identification and characterization of proSAAS, a granin-like neuroendocrine peptide precursor that inhibits prohormone processing. J. Neurosci. 20, 639–648.

Ftouhi, N., Day, R., Mbikay, M., Chrétien, M., Seidah, N.G., 1994. Gene organization of the mouse pro-hormone and pro-protein convertase PC1. DNA Cell Biol. 13, 395–407.

Fugere, M., Limperis, P.C., Beaulieu-Audy, V., Gagnon, F., Lavigne, P., Klarskov, K., Leduc, R., Day, R., 2002. Inhibitory potency and specificity of subtilase-like pro-protein convertase (SPC) prodomains. J. Biol. Chem. 277, 7648–7656.

Holland, P.M., Abramson, R.D., Watson, R., Gelfand, D.H., 1991. Detection of specific polymerase chain reaction product by utilizing the 5′–3′ exonuclease activity of *Thermus aquaticus* DNA polymerase. Proc. Natl. Acad. Sci. U. S. A. 88, 7276–7280.

Jackson, R.S., Creemers, J.W., Ohagi, S., Raffin-Sanson, M.L., Sanders, L., Montague, C.T., Hutton, J.C., O'Rahilly, S., 1997. Obesity and impaired prohormone processing associated with mutations in the human prohormone convertase 1 gene. Nat. Genet. 16, 303–306.

Jackson, R.S., Creemers, J.W., Farooqi, I.S., Raffin-Sanson, M.L., Varro, A., Dockray, G.J., Holst, J.J., Brubaker, P.L., Corvol, P., Polonsky, K.S., Ostrega, D., Becker, K.L., Bertagna, X., Hutton, J.C., White, A., Dattani, M.T., Hussain, K., Middleton, S.J., Nicole, T.M., Milla, P.J., Lindley, K.J., O'Rahilly, S., 2003. Small-intestinal dysfunction accompanies the complex endocrinopathy of human proprotein convertase 1 deficiency. J. Clin. Invest. 112, 1550–1560.

Jousan, F.D., Hansen, P.J., 2004. Insulin-like growth factor-I as a survival factor for the bovine preimplantation embryo exposed to heat shock. Biol. Reprod. 71, 1665–1670.

Jutras, I., Seidah, N.G., Reudelhuber, T.L., Brechler, V., 1997. Two activation states of the prohormone convertase PC1 in the secretory pathway. J. Biol. Chem. 272, 15184–15188.

Jutras, I., Seidah, N.G., Reudelhuber, T.L., 2000. A predicted alpha-helix mediates targeting of the proprotein convertase PC1 to the regulated secretory pathway. J. Biol. Chem. 275, 40337–40343.

Kawamura, K., Fukuda, J., Kumagai, J., Shimizu, Y., Kodama, H., Nakamura, A., Tanaka, T., 2005. Gonadotropin-releasing hormone I analog acts as an anti-apoptotic factor in mouse blastocysts. Endocrinology 146, 4105–4116.

Kurabuchi, S., Tanaka, S., 2002. Immunocytochemical localization of prohormone convertases PC1 and PC2 in the mouse thyroid gland and respiratory tract. J. Histochem. Cytochem. 50, 903–909.

Lawitts, J.A., Biggers, J.D., 1993. Culture of preimplantation embryos. Methods Enzymol. 225, 153–164.

Lee, S.N., Prodhomme, E., Lindberg, I., 2004. Prohormone convertase 1 (PC1) processing and sorting: effect of PC1 propeptide and proSAAS. J. Endocrinol. 182, 353–364.

Lighten, A.D., Hardy, K., Winston, R.M., Moore, G.E., 1997. Expression of mRNA for the insulin-like growth factors and their receptors in human preimplantation embryos. Mol. Reprod. Dev. 47, 134–139.

Lloyd, D.J., Bohan, S., Gekakis, N., 2006. Obesity, hyperphagia and increased metabolic efficiency in PC1 mutant mice. Hum. Mol. Genet. 15, 1884–1893.

Lyon, M.F., 2003. Transmission ratio distortion in mice. Annu. Rev. Genet. 37, 393–408.

Malide, D., Seidah, N.G., Chrétien, M., Bendayan, M., 1995. Electron microscopic immunocytochemical evidence for the involvement of the convertases PC1 and PC2 in the processing of proinsulin in pancreatic beta-cells. J. Histochem. Cytochem. 43, 11–19.

Marcinkiewicz, M., Day, R., Seidah, N.G., Chrétien, M., 1993. Ontogeny of the prohormone convertases PC1 and PC2 in the mouse hypophysis and their colocalization with corticotropin and alpha-melanotropin. Proc. Natl. Acad. Sci. U. S. A. 90, 4922–4926.

Marcinkiewicz, M., Ramla, D., Seidah, N.G., Chrétien, M., 1994. Developmental expression of the prohormone convertases PC1 and PC2 in mouse pancreatic islets. Endocrinology 135, 1651–1660.

Martens, G.J., Braks, J.A., Eib, D.W., Zhou, Y., Lindberg, I., 1994. The neuroendocrine polypeptide 7B2 is an endogenous inhibitor of prohormone convertase PC2. Proc. Natl. Acad. Sci. U. S. A. 91, 5784–5787.

Marzban, L., Trigo-Gonzales, G., Zhu, X.R., Rhodes, C.J., Halban, P.A., Steiner, D.F., Verchere, C.B., 2004. Role of beta-cell prohormone convertase (PC) 1/3 in processing of pro-islet antyloid polypeptide. Diabetes 53, 141–148.

Mbikay, M., Tadros, H., Ishida, N., Lerner, C.P., De Lamirande, E., Chen, A., El-Alfy, M., Clermont, Y., Seidah, N.G., Chrétien, M., Gagnon, C., Simpson, E.M., 1997. Impaired fertility in mice deficient for the testicular germ-cell protease PC4. Proc. Natl. Acad. Sci. U. S. A. 94, 6842–6846.

Mbikay, M., Seidah, N.G., Chretien, M., 2001. Neuroendocrine secretory protein 7B2: structure, expression and functions. Biochem. J. 357, 329–342.

Michaud, E.J., Bultman, S.J., Stubbs, L.J., Woychik, R.P., 1993. The embryonic lethality of homozygous lethal yellow mice (A^y/A^y) is associated with the disruption of a novel RNA-binding protein. Genes Dev. 7, 1203–1213.

Muller, L., Zhu, X., Lindberg, I., 1997. Mechanism of the facilitation of PC2 maturation by 7B2: involvement in ProPC2 transport and activation but not folding. J. Cell Biol. 139, 625–638.

Muller, L., Cameron, A., Fortenberry, Y., Apletalina, E.V., Lindberg, I., 2000. Processing and sorting of the prohormone convertase 2 propeptide. J. Biol. Chem. 275, 39213–39222.

O'Neill, C., 1998. Autocrine mediators are required to act on the embryo by the 2-cell stage to promote normal development and survival of mouse preimplantation embryos in vitro. Biol. Reprod. 58, 1303–1309.

Paquet, L., Bergeron, F., Boudreault, A., Seidah, N.G., Chretien, M., Mbikay, M., Lazure, C., 1994. The neuroendocrine precursor 7B2 is a sulfated protein proteolytically processed by a ubiquitous furin-like convertase. J. Biol. Chem. 269, 19279–19285.

Paria, B.C., Dey, S.K., 1990. Preimplantation embryo development in vitro: cooperative interactions among embryos and role of growth factors. Proc. Natl. Acad. Sci. U. S. A. 87, 4756–4760.

Peinado, J.R., Laurent, V., Lee, S.N., Peng, B.W., Pintar, J.E., Steiner, D.F., Lindberg, I., 2005. Strain-dependent influences on the hypothalamo–pituitary–adrenal axis profoundly affect the 7B2 and PC2 null phenotypes. Endocrinology.

Qian, Y., Devi, L.A., Mzhavia, N., Munzer, S., Seidah, N.G., Fricker, L.D., 2000. The C-terminal region of proSAAS is a potent inhibitor of prohormone convertase 1. J. Biol. Chem. 275, 23596–23601.

Raga, F., Casan, E.M., Kruessel, J., Wen, Y., Bonilla-Musoles, F., Polan, M.L., 1999. The role of gonadotropin-releasing hormone in murine preimplantation embryonic development. Endocrinology 140, 3705–3712.

Reese, M.G., Eeckman, F.H., Kulp, D., Haussler, D., 1997. Improved splice site detection in Genie. J. Comput. Biol. 4, 311–323.

Rehemtulla, A., Dorner, A.J., Kaufman, R.J., 1992. Regulation of PACE propeptide-processing activity: requirement for a post-endoplasmic reticulum compartment and autoproteolytic activation. Proc. Natl. Acad. Sci. U. S. A. 89, 8235–8239.

Rinchik, E.M., Tonjes, R.R., Paul, D., Potter, M.D., 1993. Molecular analysis of radiation-induced albino (c)-locus mutations that cause death at preimplantation stages of development. Genetics 135, 1107–1116.

Schäfer, M.K., Day, R., Cullinan, W.E., Chrétien, M., Seidah, N.G., Watson, S.J., 1993. Gene expression of prohormone and proprotein convertases in the rat CNS: a comparative in situ hybridization analysis. J. Neurosci. 13, 1258–1279.

Seidah, N.G., Chretien, M., 1999. Proprotein and prohormone convertases: a family of subtilases generating diverse bioactive polypeptides. Brain Res. 848, 45–62.

Seidah, N.G., Gaspar, L., Mion, P., Marcinkiewicz, M., Mbikay, M., Chrétien, M., 1990. cDNA sequence of two distinct pituitary proteins homologous to Kex2 and furin gene products: tissue-specific mRNAs encoding candidates for pro-hormone processing proteinases. DNA Cell Biol. 9, 789.

Seidah, N.G., Marcinkiewicz, M., Benjannet, S., Gaspar, L., Beaubien, G., Mattei, M.G., Lazure, C., Mbikay, M., Chrétien, M., 1991. Cloning and primary sequence of a mouse candidate prohormone convertase PC1 homologous to PC2, Furin, and Kex2: distinct chromosomal localization and messenger RNA distribution in brain and pituitary compared to PC2. Mol. Endocrinol. 5, 111–122.

Seidah, N.G., Chrétien, M., Day, R., 1994. The family of subtilisin/kexin like pro-protein and pro-hormone convertases: divergent or shared functions. Biochimie 76, 197–209.

Smeekens, S.P., Avruch, A.S., LaMendola, J., Chan, S.J., Steiner, D.F., 1991. Identification of a cDNA encoding a second putative prohormone convertase related to PC2 in AtT20 cells and islets of Langerhans. Proc. Natl. Acad. Sci. U. S. A. 88, 340–344.

Smeekens, S.P., Montag, A.G., Thomas, G., Albiges-Rizo, C., Carroll, R., Benig, M., Phillips, L.A., Martin, S., Ohagi, S., Gardner, P., Swift, H.H., Steiner, D.F., 1992. Proinsulin processing by the subtilisin-related proprotein convertases furin, PC2, and PC3. Proc. Natl. Acad. Sci. U. S. A. 89, 8822–8826.

Steiner, D.F., 1998. The proprotein convertases. Curr. Opin. Chem. Biol. 2, 31–39.

St. Germain, C., Croissandeau, G., Mayne, J., Baltz, J.M., Chretien, M., Mbikay, M., 2005. Expression and transient nuclear translocation of proprotein convertase 1 (PC1) during mouse preimplantation embryonic development. Mol. Reprod. Dev. 72, 483–493.

Takumi, I., Steiner, D.F., Sanno, N., Teramoto, A., Osamura, R.Y., 1998. Localization of prohormone convertases 1/3 and 2 in the human pituitary gland and pituitary adenomas: analysis by immunohistochemistry, immunoelectron microscopy, and laser scanning microscopy. Mod. Pathol. 11, 232–238.

Tsuji, A., Ikoma, T., Hashimoto, E., Matsuda, Y., 2002. Development of selectivity of alpha1-antitrypsin variant by mutagenesis in its reactive site loop against proprotein convertase. A crucial role of the P4 arginine in PACE4 inhibition. Protein Eng. 15, 123–130.

Ueda, K., Lipkind, G.M., Zhou, A., Zhu, X., Kuznetsov, A., Philipson, L., Gardner, P., Zhang, C., Steiner, D.F., 2003. Mutational analysis of predicted

interactions between the catalytic and P domains of prohormone convertase 3 (PC3/PC1). Proc. Natl. Acad. Sci. U. S. A. 100, 5622–5627.

Wang, H., Dey, S.K., 2006. Roadmap to embryo implantation: clues from mouse models. Nat. Rev. Genet. 7, 185–199.

Wu, G., Hao, L., Han, Z., Gao, S., Latham, K.E., de Villena, F.P., Sapienza, C., 2005. Maternal transmission ratio distortion at the mouse *Om* locus results from meiotic drive at the second meiotic division. Genetics 170, 327–334.

Yonemasu, R., Minami, M., Nakatsu, Y., Takeuchi, M., Kuraoka, I., Matsuda, Y., Higashi, Y., Kondoh, H., Tanaka, K., 2005. Disruption of mouse *XAB2* gene involved in pre-mRNA splicing, transcription and transcription-coupled DNA repair results in preimplantation lethality. DNA Repair 4, 479–491.

Yu, P., Ma, D., Xu, M., 2005. Nested genes in the human genome. Genomics 86, 414–422.

Zheng, M., Streck, R.D., Scott, R.E., Seidah, N.G., Pintar, J.E., 1994. The developmental expression in rat of proteases furin, PC1, PC2, and carboxypeptidase E: implications for early maturation of proteolytic processing capacity. J. Neurosci. 14, 4656–4673.

Zhou, A., Bloomquist, B.T., Mains, R.E., 1993. The prohormone convertases PC1 and PC2 mediate distinct endoproteolytic cleavages in a strict temporal order during proopiomelanocortin biosynthetic processing. J. Biol. Chem. 268, 1763–1769.

Zhu, Q., Lindenbaum, M., Levavasseur, F., Jacomy, H., Julien, J.P., 1998. Disruption of the NF-H gene increases axonal microtubule content and velocity of neurofilament transport: relief of axonopathy resulting from the toxin beta,beta′-iminodipropionitrile. J. Cell Biol. 143, 183–193.

Zhu, X.R., Orci, L., Carroll, R., Norrbom, C., Ravazzola, M., Steiner, D.F., 2002a. Severe block in processing of proinsulin to insulin accompanied by elevation of des-64,65 proinsulin intermediates in islets of mice lacking prohormone convertase-1/3. Proc. Natl. Acad. Sci. U. S. A. 99, 10299–10304.

Zhu, X.R., Zhou, A., Dey, A., Norrbom, C., Carroll, R., Zhang, C.L., Laurent, V., Lindberg, I., Ugleholdt, R., Holst, J.J., Steiner, D.F., 2002b. Disruption of PC1/3 expression in mice causes dwarfism and multiple neuroendocrine peptide processing defects. Proc. Natl. Acad. Sci. U. S. A. 99, 10293–10298.